Hindawi Publishing Corporation
Advances in Optical Technologies
Volume 2013, Article ID 314906, 13 pages
http://dx.doi.org/10.1155/2013/314906

Research Article

In Search of Early Time: An Original Approach in the Thermographic Identification of Thermophysical Properties and Defects

Daniel L. Balageas[1,2]

[1] *Composite Materials and Systems Department, ONERA, BP 72, 92322 Châtillon Cedex, France*
[2] *TREFLE Department, ENSAM, Institute of Mechanics and Engineering of Bordeaux (I2M), Esplanade des Arts et Métiers, 33405 Talence Cedex, France*

Correspondence should be addressed to Daniel L. Balageas; daniel.balageas@u-bordeaux1.fr

Received 11 August 2012; Accepted 25 November 2012

Academic Editor: Carlo Corsi

Active thermography gives the possibility to characterize thermophysical properties and defects in complex structures presenting heterogeneities. The produced thermal fields can be rapidly 3D. On the other hand, due to the size of modern thermographic images, pixel-wise data processing based on 1D models is the only reasonable approach for a rapid image processing. The only way to conciliate these two constraints when dealing with time-resolved experiments lies in the earlier possible detection/characterization. This approach is illustrated by several different applications and compared to more classical methods, demonstrating that simplicity of models and calculations is compatible with efficient and accurate identifications.

1. Introduction

The evolution of thermophysical properties metrology and nondestructive evaluation (NDE) is characterized by the increased use of refined inverse techniques [1] requiring the establishment of models taking into account many parameters, although among these parameters often only one parameter is of interest for the experimenter. This complexity is particularly important when the analyzed thermal fields are 3D, a situation characteristic of the experiments realized with thermographic systems producing sequences of large thermal images of complex structures presenting important heterogeneities in their thermal properties, internal geometries, and boundary conditions. This approach leads to time-consuming calculations that may be prohibitive for thermographic data processing. Furthermore, it happens that in many situations the reality remains more complex than the sophisticated model used.

How to conciliate the existence 3D thermal situations involving numerous parameters and the necessity to have rapid calculations compatible with the very high number of information to process in a thermographic image sequence?

A solution lies in the use of 1D thermal models for pixel-wise data processing and the choice of a limited early time domain (for time-resolved techniques) or high frequency domain (for modulated techniques) for which the measured temperatures are essentially depending on the sole parameter to be identified and weakly affected by the 3D heat transfer. To achieve that, the proposed approach consists in performing the identification at the earlier possible time (or at the higher possible frequency) after the thermal stimulation. Here, we will mainly consider time-resolved techniques and early time detection (emerging signal).

The present work wants to show the following.

(i) A detailed procedure can be defined for early detection and characterization (see Section 2).

(ii) That this approach is not new. In a first step, it has been applied in the field of thermophysical properties measurements (period 1970–1990). This review is the subject of Section 3.

(iii) The application to NDE, started at the beginning of the 90's, continues to give rise to new developments (Section 4).

The goal of the present work is to put into perspective results spread over three decades, showing the unity of the approaches up to now hidden by the diversity of the applications and to emphasize that in thermal methods precociousness is as important as signal-to-noise ratio.

2. Presentation of the Early Detection Approach

The early detection approach can be considered as the sequence of the following six operations:

(i) choice of a model simpler than the actual configuration, generally 1D,

(ii) choice of an early time window for the analysis of the thermograms, in such a way that very few parameters (one if possible) be influent,

(iii) inverse problem solving in these conditions,

(iv) Analysis of the time evolution of the so-identified parameter for the assessment of its accuracy,

(v) choice of a fitting function,

(vi) extrapolation to zero time (thermophysics application) or zero contrast (NDE) for obtaining the most precise parameter estimate.

Most of the examples that will be given consider models with only one parameter to be identified. Nevertheless, more complex situations are possible. The second example of Section 3 presents a model in which three parameters are to be identified. Consequently the procedure is more complex, involving two time window analysis and time extrapolations followed by two space extrapolations thanks to the use of several samples of different thicknesses.

3. Application in the Field of Thermophysical Properties Measurements

The early detection approach defined in Section 2 is illustrated in Section 3.1 in the case of a simple configuration (rear face flash diffusivity experiment), universally known under the name of Parker's method [2], applied to the diffusivity measurement of an homogeneous slab.

In Section 3.2, a more complex procedure is presented dealing with the same type of experiment (rear face flash diffusivity), identifying the *in situ* diffusivities of the components (matrix and reinforcement) of a 3D C/C composite and the thermal contact resistance characterizing the interface between them.

3.1. Rear Face Flash Diffusivity Measurement. In flash thermal diffusivity measurements on the face opposite to the pulsed heat deposition the sample heat losses distort the rear face temperature time history. These thermal losses occurring necessarily after the flash, the temperature is all the less disturbed as time is nearer the origin. Consequently, the diffusivity identification by extrapolating towards the initial time the apparent diffusivity-versus-time history resulting from the use of an adiabatic solution was proposed in 1982 [3, 4]. It was demonstrated that the early phase of the thermogram (for instance for a defect Fourier number $\mathrm{Fo}_d = \kappa t/z_d^2 < 0.1$, where κ is the diffusivity of the material and z_d the defect depth) may be used for this early detection if an estimate of the final adiabatic temperature increase, ΔT_{lim}, is deduced without any assumption concerning the heat losses from the maximum temperature reached with losses, ΔT_{max}. A relation between these two parameters was proposed

$$\mathrm{Log}_{10}\left[\mathrm{Log}_{10}\left(\frac{\Delta T_{\mathrm{lim}}}{\Delta T_{\mathrm{max}}}\right)\right] = -\frac{0.667 t_{\mathrm{max}}}{t_{1/2}} + 1.113, \quad (1)$$

where t_{max} and $t_{1/2}$ are, respectively, the measured occurrence times of the maximum and half maximum temperature increase at the center of the sample. This relation allows to normalize the thermogram: $\Delta T(t)/\Delta T_{\mathrm{lim}} = (\Delta T(t)/\Delta T_{\mathrm{max}}) \times (\Delta T_{\mathrm{max}}/\Delta T_{\mathrm{lim}})$, and using a look-up table to build an apparent diffusivity curve, $\kappa(t)$, from the analytical solution for the 1D rear face adiabatic sample submitted to a pulsed stimulation. Whatever is the accuracy of the estimated ΔT_{lim}, it was verified that the law $\kappa(t)$ starts at $t = 0$ from the actual diffusivity value, and that if the estimation is sufficiently accurate, the apparent diffusivity evolution in the early times ($\mathrm{Fo}_d < 0.1$) can be approximated by a parabolic law whose peak is obtained for $t = 0$. To improve the accuracy of the parabolic fitting using least mean squares, the experimental points were weighted by the accuracy of the diffusivity measurement deduced from the a sensitivity analysis. It was imposed to the parabola to have a zero slope at $t = 0$.

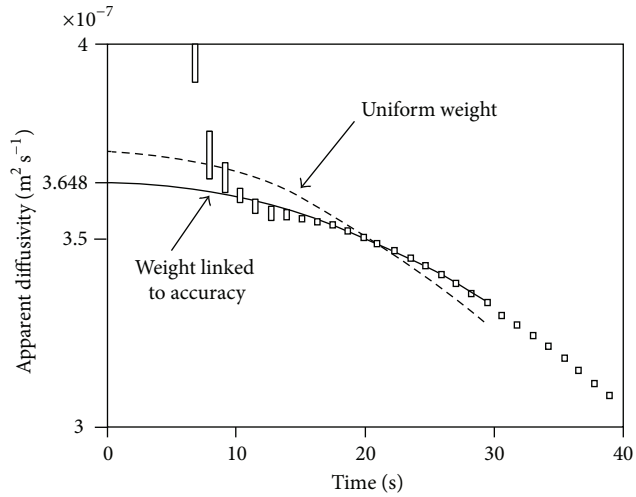

Figure 1: Test no. 2 on plaster identified apparent diffusivity law and regression parabola with a uniform weight and with a nonuniform weight linked to the accuracy of the measurement, taken from [4].

Figure 1 presents, taken from [4], the extrapolation in the case of a measurement on a 10 mm thick disk-shaped plaster sample, with a radius over thickness ratio $R/L = 1.206$. An extrapolated value of diffusivity is found $3.65 \cdot 10^{-7}\ \mathrm{m^2 s^{-1}}$.

Table 1 summarizes the diffusivity results obtained by this method and compares them to results obtained with exactly the same samples by three methods (round robin tests) as follows.

Table 1: Present method result and comparison to Parker's and Degiovanni's methods.

Material	Test number	Sample		Identified diffusivity ($m^2\ s^{-1}$) $\times 10^7$					
		Thickness (mm)	R/L	Parker's method	Degiovanni [5]			Degiovanni [6]	Balageas [4]
					$\kappa_{2/3}$	$\kappa_{1/2}$	$\kappa_{1/3}$		
Plaster	#1	9.96	1.206	4.759	3.675	3.703	3.689	3.69	**3.703**
Plaster	#2	9.96	1.206	4.734	3.618	3.644	3.645	3.64	**3.648**
Chalk	#3	6.16	1.950	3.548	2.861	2.881	2.886	2.89	**2.905**

(i) The Parker's formula, $\kappa = 0.139\, L^2/t_{1/2}$, with $t_{1/2}$ the half rise time, which considers the sample adiabatic and leads to considerable errors due to the low conductivities of the three materials chosen for the tests.

(ii) The more precise method at the time of the publication of the present method: the partial times method of Degiovanni [5]. The method of partial times considers for the identification several pairs of points of the thermogram corresponding to the following normalized temperature increases $\Delta T(t)/\Delta T_{\max}$: 1/3 and 5/6, 1/2 and 5/6, 2/3 and 5/6. It is interesting to compare the Degiovanni's method with the present early detection approach because, as shown in Figure 2, the extrapolation method results are coherent with the evolution with time of the identified diffusivities of the points considered in the data processing of the Degiovanni's partial times method. We see that the present method corrects the bias of this method, which increases with identification times.

(iii) The method of partial moments, proposed by Degiovanni [6] that is still considered as a reference. There is a perfect agreement with this method. The results of the partial moments are not plotted in Figure 2 because they would not be distinguishable from those of the present method.

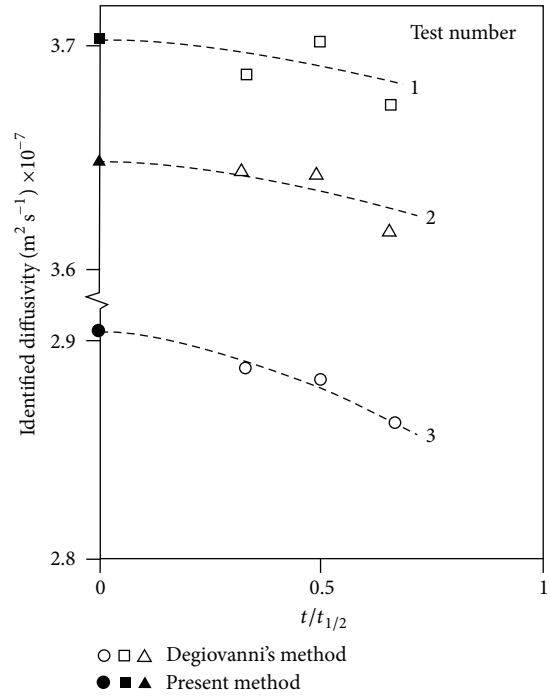

Figure 2: Compared results of Degiovanni's partial times method and present method, taken from [4].

3.2. Rear Face Flash Measurement of the In Situ Diffusivities of the Components of Periodic Directional-Reinforced Composites

3.2.1. Periodic Directional Reinforced Composites (PDRCs). The types of materials here considered are PDRCs (periodic directional reinforced composites) in which the reinforcement is arranged following preferential directions. For instance, unidirectional carbon/epoxy composites and 3D carbon/carbon composites belong to this family of materials and the identification method here presented can be applied to them. These materials are difficult to homogenize when there is a large difference between the thermal conductivities of the composite components (matrix and reinforcement) and when the main heat transfer is parallel to a reinforcement direction [7].

Considering the same type of measurements as in the previous section (rear face flash diffusivity), a more complex procedure is presented, which identifies the *in situ* diffusivities of the matrix and reinforcement and the thermal contact resistance characterizing the interface between them in the case of a 3D C/C composite [8–10]. The method supposes that the composite sample is quasi adiabatic (no heat losses).

The simplest PDRCs that can be imagined are presented in Figure 3. They are unidirectional PDRCs. The two components are arranged in alternated slabs parallel to the imposed heat flux (Figure 3(a)) or following a chessboard pattern (Figure 3(b)). The dimensional geometric parameters are the space period of the pattern, ω, the thickness of the medium, L, and the volume ratio of the components (τ_i). For these first two composites $\tau_1 = \tau_2 = 0.5$. The more thermally conductive component is supposed to be the reinforcement, since it is usually the case (i.e., in C/epoxy or C/C composites).

A slightly more general arrangement for 1D PRDC is given in Figure 4(a). Figure 4(b) corresponds to a more realistic arrangement representative of carbon/epoxy composite and Figure 4(c) to a 3D C/C material with orthogonal x, y, z reinforcements.

Based on numerous numerical simulations [9], it has been demonstrated that the transient thermal behavior of 1D

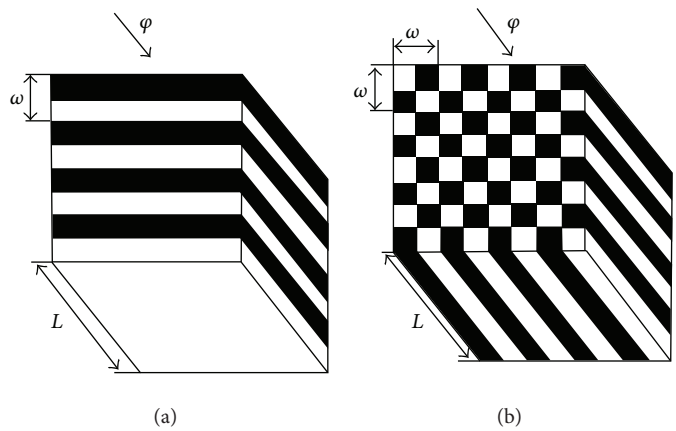

Figure 3: Simple configurations of unidirectional PDRCs: (a) stack of parallel layers, (b) chessboard pattern (from [9]).

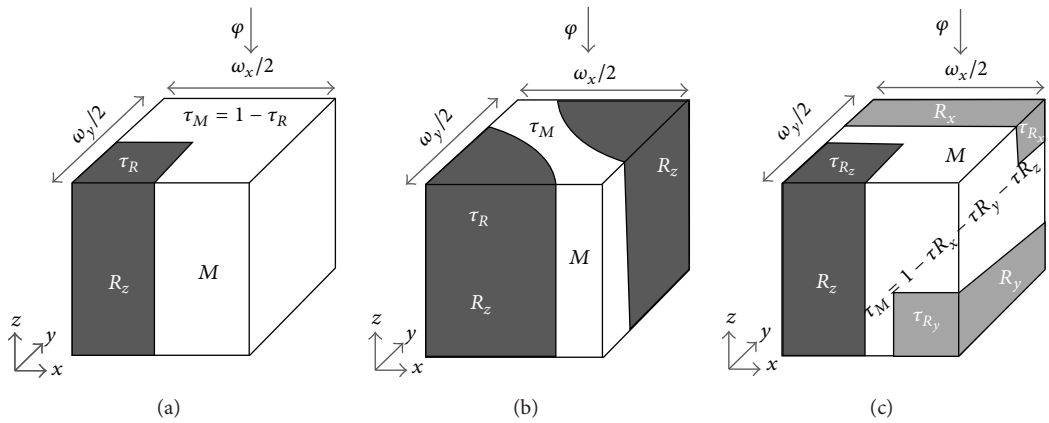

Figure 4: (a) Model of the elementary volume (1/4 of the repetitive cell) of a 1D PDRC, (b) idem for a 1D C/epoxy composite, (c) idem for a 3D C/C with x, y, z orthogonal reinforcements, from [10, 11].

PDRCs, when considering the mean temperature evolution, $\overline{T}(t)$ depends only on five nondimensional parameters:

(i) volume content of the reinforcement, τ_R;

(ii) the reinforcement-to-matrix ratio of thermal conductivities, $k_{R/M} = k_R/k_M$;

(iii) the reinforcement-to-matrix ratio of volume specific heats, $C_{R/M} = C_R/C_M$;

(iv) the specific contact surface between reinforcement and matrix per unit surface of composite: $\sigma = L\Sigma$, where L is the sample thickness, and Σ the specific contact surface between reinforcement and matrix per unit volume, parameter which depends on the shape of the section of the reinforcement;

(v) the specific contact thermal resistance between reinforcement and matrix: $\rho = Rk_M\Sigma$, R being the contact thermal resistance of the interface.

This mean temperature $\overline{T}(t)$ is easily measured by using IR radiometer or thermography if the emissivity of the surfaces are homogenized by a black coating insuring uniform emissivity.

3.2.2. Principle of the Identification of the Reinforcement Diffusivity and Homogenized Diffusivity from the Time Evolution of the Rear Face Mean Temperature $\overline{T}(t)$ in the Case of 1D DRC. Let us consider a 1D PDRC with a periodic pattern such as those of Figures 4(a) and 4(b). A typical mean temperature evolution of the rear face of the sample in flash diffusivity measurement is given in Figure 5(a) and compared to the theoretical response of a homogeneous material.

At the beginning, the energy that arrives at the rear face of a sample of thickness L has travelled through the more conductive component of the PDRC, here the reinforcement. If the identification is performed for each and every points of the curve, the identified diffusivity varies with time and the earlier the considered point, the nearer of the reinforcement diffusivity it is. Thus, following the early detection approach,

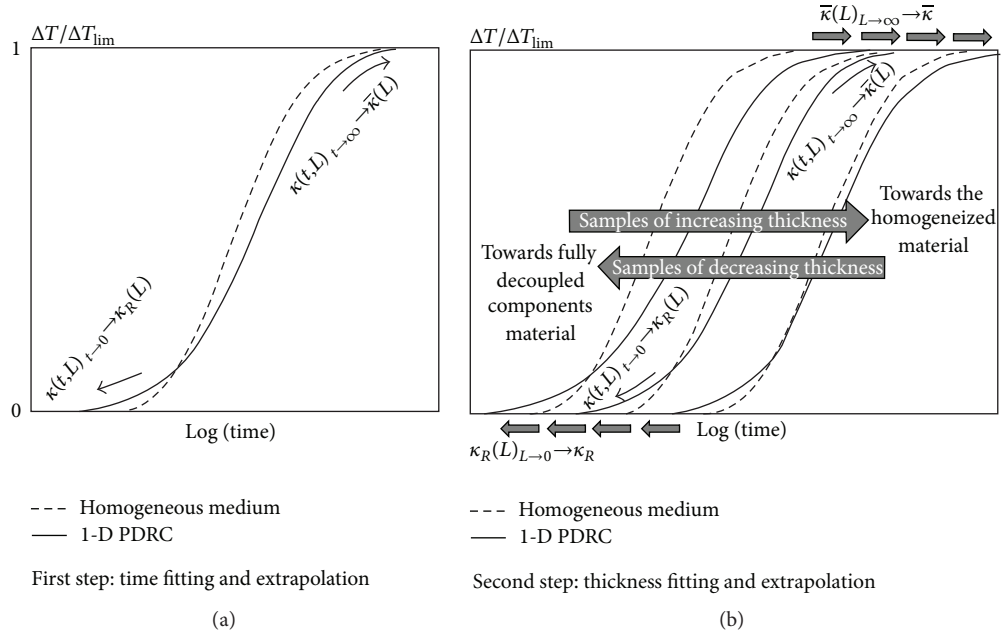

FIGURE 5: *In situ* characterization of a 1D PDRC. Principle of the early time and later time identifications (a), followed by spatial extrapolations to zero and infinite sample thicknesses (b).

by fitting the early part of the apparent diffusivity law and extrapolating it to zero time, an estimate of the reinforcement diffusivity is reached. This diffusivity is depending on L

$$\kappa(t,L)_{t\to 0} \longrightarrow \kappa_R(L). \tag{2}$$

Using several samples of different thicknesses the law $\kappa_R(L)$ can be extrapolated to zero thickness and the so-extrapolated diffusivity can be considered as the best possible estimate of the reinforcement diffusivity

$$\kappa_R(L)_{L\to 0} \longrightarrow \kappa_R. \tag{3}$$

On the contrary, the energy arriving at the end of the experiment can be considered as representative of a partially homogenized material. In effect, for long times, 3D heat transfers have enough time to become important and homogenize the temperature of the two components (reinforcement and matrix). These 3D effects, which are generally considered as a disturbing phenomenon, have in the present case a beneficial role, becoming a source of information about the material. The identified diffusivity law presents a final asymptote that can be considered as an approximate estimate of the fully homogenized material

$$\kappa(t,L)_{t\to\infty} \longrightarrow \overline{\kappa}(L). \tag{4}$$

Thanks to the series of measurements performed with the different samples of various thicknesses, the law of partially homogenized diffusivity versus thickness can be extrapolated to an infinite thickness and the so-extrapolated value can be considered as the best estimate of the diffusivity of the fully homogenized material equivalent to the composite

$$\overline{\kappa}(L)_{L\to\infty} \longrightarrow \overline{\kappa}. \tag{5}$$

In a third step, with a few assumptions which depends on the considered composite, from κ_R and $\overline{\kappa}$, it is possible to deduce the value of the diffusivity of the less conductive component (generally the matrix), κ_M, and the thermal resistance, R, characterizing the interface between the two components (see in particular [10, 12, 13]).

3.2.3. Application to 3D C/C Composites. The method has been applied to two 3D C/C composites in which the reinforcement is constituted of bundles of carbon fibers highly anisotropic and highly axially conductive, oriented in the three Cartesian directions x, y, z.

The first step consists to consider the 1D PDRC model of Figure 4(a) as an approximation equivalent to the 3D PDRC of Figure 4(c) in the case of the 3D C/C composite, considering that, due to the anisotropy of the reinforcement and the same chemical nature of the matrix and the reinforcement, it is possible to replace the actual matrix and the transverse reinforcement (following x and y directions) by an equivalent matrix. The identification procedure of Section 3.2.2 is then applied to this 1D PDRC. The operation can be repeated with the two other orientations of the samples to obtain the diffusivity of the three reinforcements if the composite is not equilibrated.

Figure 6 presents the experimental thermograms obtained for the 3D C/C no. 3 the flux being parallel to the z-reinforcement. They are compared to the thermograms of the equivalent homogenized material with the identified homogenized diffusivity, $\overline{\kappa}$, and the thermograms calculated using the equivalent 1D PDRC model with the identified parameters. The identified parameters are presented in Table 2 for two materials (3D C/C no. 1 and 3D C/C no. 3 for two orientations). These results show that even for a coupon

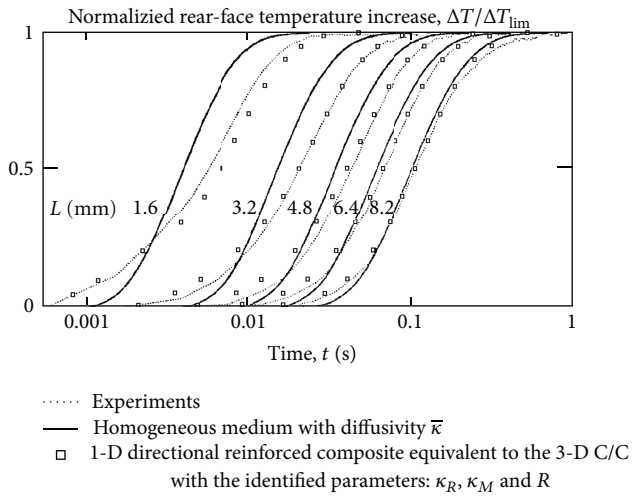

Figure 6: Normalized experimental pulse diffusivity rear face thermograms (mean temperature) obtained with a series of 3D C/C coupons of different thicknesses. Comparison to the homogeneous medium solution with the identified homogenized diffusivity, $\overline{\kappa}$, and to the 1D directional reinforcement composite equivalent to the 3D C/C using the identified parameters: axial thermal diffusivity of the reinforcement, κ_R, diffusivity of the matrix, κ_M, and thermal contact resistance of the reinforcement/matrix interface, R. Taken from [10, 13].

thickness of 8.2 mm, the material transient behavior is not exactly that of a homogeneous material. This thickness, knowing that the z-space period is 0.8 mm, represents ten times the space period.

These results were obtained with an IR radiometer viewing an area of the rear face much larger than a mesh of material to obtain a mean temperature measurement. It could be easily performed with an IR camera.

The main merit of the method is the fact that the measured properties are relative to *in situ* materials, which is of prime importance since the material process has a strong influence on the resulting final thermal properties of the product, in particular the axial diffusivity of the reinforcement.

3.2.4. Complementarity of Front-Face and Rear Face Pulse Measurements. The front-face and rear face pulse experiments are complementary [14]. In effect, let us apply the zero-time extrapolation to the apparent diffusivity identified from the rear face mean-temperature time evolution (see Figure 7(a)) and to the apparent effusivity identified from the front-face mean-temperature time evolution (see Figure 7(b)). These operations permit, respectively, the identification of characteristic thermal properties of the reinforcement parallel to the flux (longitudinal diffusivity) and of the equivalent matrix resulting from the homogenization of the matrix (isotropic effusivity) and of the two reinforcements perpendicular to the heat flux (radial effusivity). In other words, at the beginning of the pulse experiments, on the front-face the heating is driven by the less conductive component of the composite and on the rear face by the more conductive component.

4. Application to Nondestructive Evaluation (NDE)

4.1. Notion and Interest of the Emerging Contrast. For NDE, the experimental data from which defect parameters can be identified are not thermograms (temperature increase, a function of time: $\Delta T(x, y, t) = T(x, y, t) - T(x, y, t = 0)$) but the time evolution of the contrasts between the temperature rise of a defective zone and the one of a sound zone taken as a reference, $Cr(x, y, t) = (\Delta T(x, y, t)_d - \Delta T(x, y, t)_s)/\Delta T(x, y, t)_s)$. Consequently, the early detection approach in NDE consists in exploiting the contrast when it is just emerging from the noise, reason why we proposed to call it "the emerging contrast." Figure 8 presents the principle of the detection of the emerging contrast.

This attitude is contrary to common practice. In effect, traditionally, pulse thermography users favored the maximum contrast to identify the depth and thermal resistance of defects, starting from the *a priori* justified reason that it corresponds to the best SNR. This choice, which could be understood when the performances of cameras were limited (NETD $\geq$ 100 mK), is unfortunate and inappropriate. Nevertheless, it is still used by most of the users of the pulse technique. The early detection approach by the use of the emerging contrast is an efficient alternative that deserves to be promoted, as it will be demonstrated here.

4.1.1. "Universality" of the Emerging Contrast (Pulse Thermography). Let us consider the simple 1D configuration of a thermally imperfect interface (thermal resistance) inside two layers of solid materials. The interface is characterized by an extrinsic parameter, its location depth, z_d, and by an intrinsic thermal property, its thermal resistance, R_d. If $R_d = 0$, the structure is considered as sound and if $R_d > 0$, it is considered as being defective, with a resistive defect which has to be detected and characterized.

The problem is that the time-evolution of Cr depends on a large number of factors: the depth z_d, the thermal resistance, R_d, but also the total thickness of the structure, L, the thermal properties of the two layers effusivities and diffusivities, and the boundary conditions characterized by heat transfer coefficients h.

Figure 9 presents the wide variety of contrast evolutions that can be encountered. These data are the synthesis of simulation results taken from [15]. All parameters are non-dimensional and the graph is in log-log scales to conveniently show the various time scales. The possible domain in which the contrast may evolve, here lightly coloured in grey, is enormous, and it is obvious that to solve the inverse problem it is necessary to rely on a model taking into consideration all the aforementioned parameters.

A simple explicit expression relating the time of occurrence and the amplitude of the maximum relative contrast, a universally known and used approach, cannot be *a priori*

Table 2: *In situ* identified thermal properties of two 3D C/C composites, taken from [10].

Identified thermal parameters	Materials		
	3-D C/C no. 1	3-D C/C no. 3 //	3-D C/C no. 3 ⊥
Mean volume heat capacity[a]			
$\overline{c}$ (MJ m^{-3} K^{-1})	1.4	1.4	1.4
Homogenized properties			
$\overline{\kappa}$ (cm^2 s^{-1})	1.09	0.90	1.06
$\overline{k}$ (W m^{-1} K^{-1})	154	127	149
Reinforcement//heat flux			
κ_R (cm^2 s^{-1})	3.0	2.6	3.1
k_R (W m^{-1} K^{-1})	423	366	437
Equivalent matrix			
κ_M (cm^2 s^{-1})	0.27	0.33	0.48
k_M (W m^{-1} K^{-1})	38	46	68
Reinforcement/matrix interface			
ρ	0.01	1.6	6.6
R (m^2 K W^{-1})	$2.0{\cdot}10^{-7}$	$2.8{\cdot}10^{-5}$	$5.7{\cdot}10^{-5}$

[a] Estimated value.

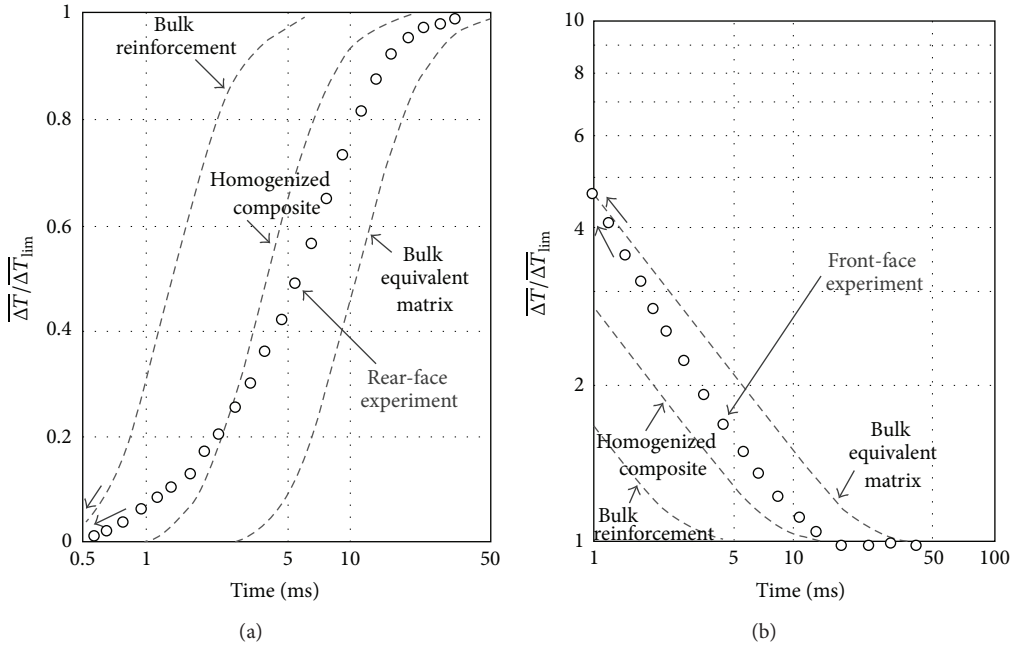

Figure 7: Compared mean temperature time histories of the front- and rear faces in the case of the 3D C/C #3// and comparison to the calculated thermograms corresponding to the thermal properties of the bulk reinforcement (longitudinal properties), bulk equivalent matrix, and fully homogenised composite, taken from [14].

satisfying when one considers the wide scatter existing on these two parameters.

Nevertheless, the main lesson which can be drawn from this graph is the existence, at the origin, of a narrow tail-shaped domain in which all curves merge, thus where a unique correlation between the relative contrast Cr and the defect Fourier number Fo_d can be used for the identification of the defect depth whatever is the thermal resistance and the other already mentioned parameters.

If we suppose that one can evaluate the occurrence time of a contrast of 1%, the maximum error on the identified depth is ±7%. Of course an earlier identification, based on a still lower contrast, leads to a more precise identified depth. The aim to be reached is clear; the problem is in the way to practically achieve the required experimental accuracy.

This simple example illustrates the main virtue of the emerging contrast: the "universality" of its applicability.

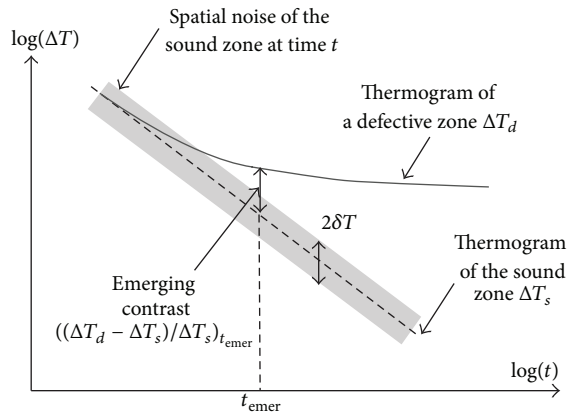

Figure 8: Principle of the detection of the emerging contrast.

Another illustration of this universality is given by the following study of the characterization of a defect embedded at different depths in a slab of a homogeneous sample. Let us consider a slab of thickness L, with a 1D defect located at the depth z_d and characterized by a thermal resistance R_d. For such a defect embedded in a semi-infinite medium, the thermal contrast associated with the 1D defect is depending on two non dimensional parameters: the Fourier number related to the defect depth, $Fo_d = \kappa t/z_d^2$, and the non dimensional thermal resistance $R^* = R_d/(z_d/k)$, the ratio of the defect thermal resistance to the one of the material layer in between the defect and the front-surface (see for instance [16, 17]. In these expressions, κ and k are, respectively, the diffusivity and the thermal conductivity of the material in between the monitored surface and the defect. In the case of a slab, the situation is more complex as seen in Figure 10(a). This Figure presents the Fourier-evolution of the relative contrast for various values of the normalized defect depth, z_d/L, and for $R^* = 1$. Similar (but different) nets would be obtained for other values of this last parameter. The shape of the contrast curves presents a maximum highly dependent on R^* and z_d/L parameters. The influence of the rear face "echo" gains in importance with increasing z_d/L and drastically decreases the amplitude of the relative contrast when the defect is approaching from this rear face, making the detection more and more problematic. Like in Figure 9, the large spreading of the net is converging to a narrow "tail" in which all curves merge for early times when the contrast is emerging form the noise. Thus, considering the emerging contrast domain ($Fo_d < 0.5$ and Cr of a few percents), for identification purpose, we can use the unique curve Cr (Fo_d, $R^* = 1$) corresponding to the case of the defect embedded in a semi-infinite medium, for which there is no rear face reflection (see Figure 10(b)).

4.1.2. Identification Based on Emerging Contrast Needs Simpler Model than That Based on Maximum Contrast. Figure 10(b) presents the emerging contrast domain taken from Figure 10(a) and compares the contrast curves net to the two grey dotted curves of relative contrast related to the defects of infinite thermal resistance and $R^* = 1$ in a semi-infinite medium, curves taken from [19, 20]. We see that this second curve remains near of the curves of the net for contrast of a few percents when z_d/L is smaller than 0.8. This means that we can use the semi-infinite medium solution Cr (Fo_d, R^*) for identifying the depth and thermal resistance of a defect in this early time domain, instead of using a Cr (Fo_d, R^*, z_d/L) function.

4.1.3. Early Detection and Characterization Lead to Less Blurred Images and More Accurate Identified Defect Parameters. Both Figures 9 and 10 show that the gain in precociousness of the identification when going from maximum contrasts to emerging contrasts can be very important (up to one order of magnitude). This gain is important since less time is given to 3D internal heat diffusion effects. This means from a qualitative point of view that the defect images will be less blurred, an important quality that increases the detectivity of the method, and quantitatively this produces a gain in accuracy for the identified parameters. This has been demonstrated in [19, 20].

4.2. Rapid Survey of the Early Detection and Characterization Approach in the NDE Literature. At the beginning of the 90's, the attention of several authors was drawn to the fact that it would be better to consider the contrast at its beginning to achieve an early detection.

The idea of an early identification of the defect depth, z_d, from the emerging contrast time was first formulated by Bontaz [21, 22] who proposed the following empirical relation:

$$t_0 = \frac{z_d^2}{2\pi\kappa}, \tag{6}$$

where t_0 is the origin time of the contrast, called by the authors the "divergence" time. This relation can be formulated using the defect Fourier number

$$Fo_d = \frac{\kappa t_0}{z_d^2} = \frac{1}{2\pi} = 0.159. \tag{7}$$

The weakness of this approach was double: (i) the relation between defect depth and divergence time was totally empirical and no precise procedure was proposed since the emergence had to be localized by the simple examination of the contrast curve without any indication given concerning the relative contrast value to consider for this determination of t_0; (ii) for the thermal resistance, R_d, the identification was similar to the temporal moment approach already proposed for diffusivity identification by Degiovanni [6], and for defect characterization by Balageas et al. [23], and was based on the use of the time integral of the full contrast from its origin to its extinction, then comprising data related to high Fourier numbers and consequently corrupted by 3D conduction effects.

Finally, Krapez et al. [18, 24, 25] kept the idea of performing the identification as early as possible with the emerging contrast, but developed a precise methodology

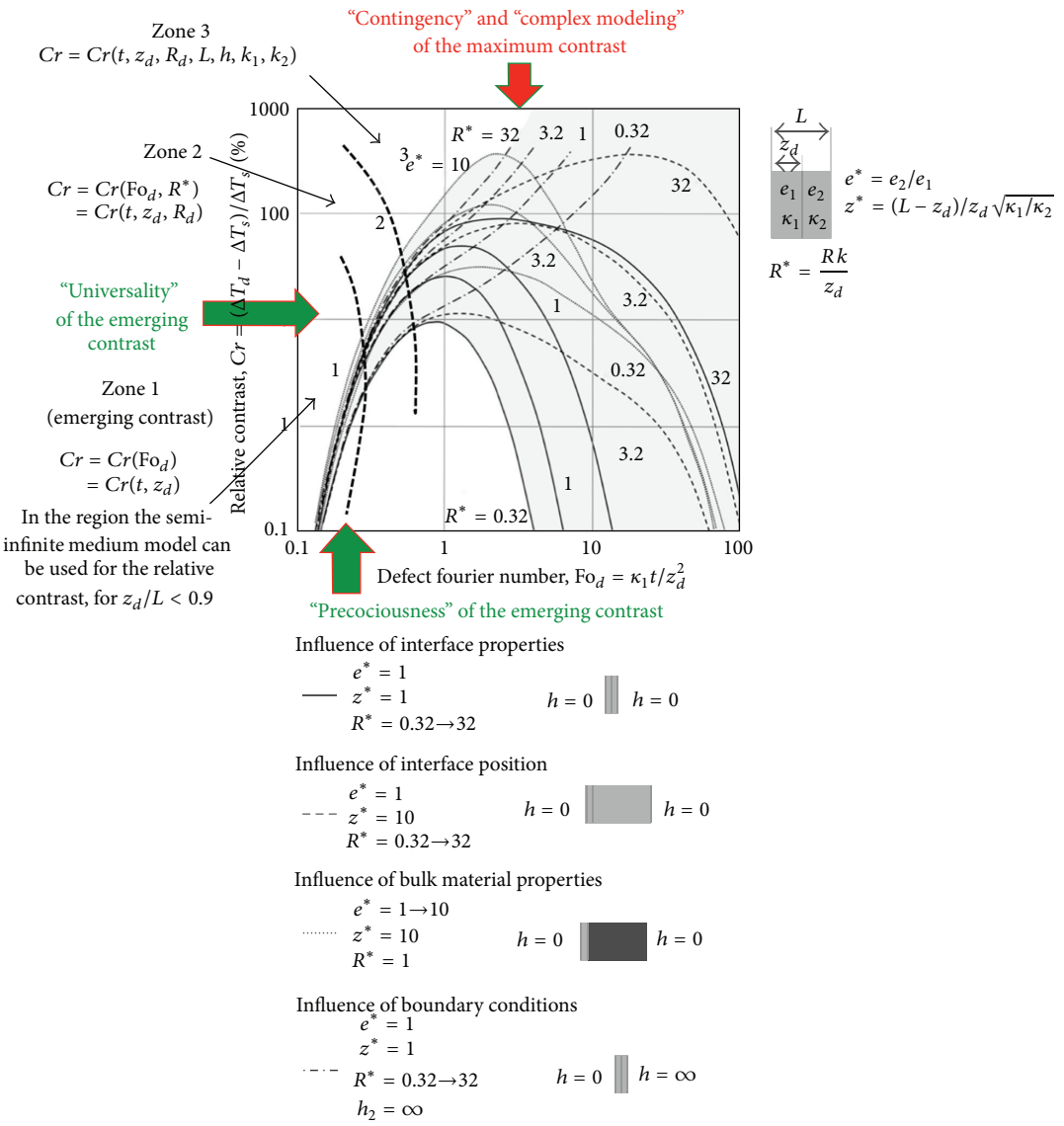

FIGURE 9: The virtues of the emerging contrast: universality, precociousness, and simple modeling. Comparison to the maximum contrast.

for the identification leading to propose explicit analytical formulas for identifying both depth and thermal resistance of a defect

$$z_d = \sqrt{\kappa_z t \mathrm{Ln}\left[\frac{2}{\mathrm{Cr}(t)}\right]},$$
$$R_d = \frac{\mathrm{Cr}(t)\,\kappa_z t/k_z z_d}{\exp\left(-z_d^2/\kappa_z t\right) - \mathrm{Cr}(t)/2}, \quad (8)$$

expressions in which Cr(t) is the relative contrast measured at time t, and k_z and κ_z are, respectively, the thermal conductivity and thermal diffusivity of the material between the monitored surface and the defect. The identification was achieved in two steps. The first relation was used for relative contrasts near of 1 to 3% and once the defect depth identified, the second formula was used for identifying the thermal resistance for slightly larger contrast (3 to 6%).

In parallel to this research, another way to perform early detection was explored. Almond et al. [26, 27] found from numerical simulations and from experiments on a sample with artificial defects of same thermal resistance, located at the same depth, but with different sizes, that the "thermal contrast slope at the beginning" was independent of the size of the defect and just related to the defect depth. He suggested that the "short-time slope" of the contrast-time curve can be used to assess the defect depth rather than the peak time (time of the maximum contrast). Thomas, Favro and coll [28–30], and Ringermacher et al. [31] proposed to use the time of occurrence of the "peak slope" of the contrast to identify the

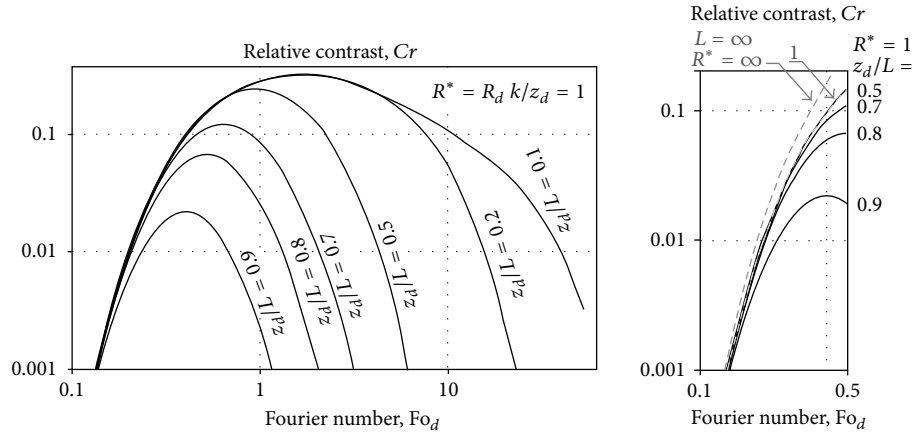

(a) Sample finite thickness effect on the relative contrast

(b) Emerging contrast domain

FIGURE 10: On the left: Influence of the normalized defect depth, z_d/L, on the relative contrast generated by a defect of normalized thermal resistance $R^* = 1$ in a slab of thickness L. On the right: Comparison in the emerging contrast domain between the contrasts generated by the same defect in a semi-infinite medium (solution used for the depth and thermal resistance identification by the early detection technique) and in a slab of thickness L.

defect depth. This proposal remained qualitative, no explicit relation relating the defect depth to this time being proposed by these authors.

Recently, Sun [32] studied quantitatively the relation between the contrast slope peak time, t_{ps}, and the defect depth using a normalized time $\omega_{\text{def}} = \pi^2 Fo_{\text{def}} = \pi^2 \kappa t_{\text{ps}}/z^2$ def. His study, limited to the case of an infinite defect thermal resistance (case of a hole machined in a slab), shows that the maximum slope is reached for a $Fo_{\text{def}} = 0.368$, which allows to identify the defect depth

$$z_d = 1.65\sqrt{\kappa t_{\text{ps}}}. \quad (9)$$

Nevertheless, this relation is only valid when the relative depth (ratio of the defect depth to the total sample thickness) is lower than 0.5. For higher values, the characteristic Fourier number is a strong function of the normalized defect depth, decreasing continuously down to 0.25 for a defect approaching the sample rear face.

This approach, although constituting a progress compared to the use of the occurrence time of the maximum contrast, is not as interesting as the early detection from the emerging contrast because the contrast slope peak occurs later than the emergence of the contrast ($Fo_{\text{def}} = 0.368$ instead of $Fo_{\text{def}} = 0.159$ for the Bontaz method, see (7)).

4.3. Recent Developments in Early Detection and Characterization of Defects

4.3.1. Improvement of the Emerging Contrast Technique by Linear Extrapolation to Nill Contrast. Balageas [19, 20] recently reworked the method developed in the 90's [18, 24, 25], following rigorously the early detection procedure described in Section 2 and using the identification formulas (8). In particular, he proposed and experimentally validated the extrapolation to zero contrast of the law of the identified defect depth as a function of the contrast. By this way, the most accurate estimate of the defect depth is obtained. A relation between the error on the so-identified defect depth and the value of the defect thermal resistance is found, allowing to correct the first estimate of the defect depth once estimated the thermal resistance, which improves the accuracy of the method.

The early detection approach using the described procedure allows to reach the optimum accuracy on both the depth and the thermal resistance of defects: between 0.1% and 10% for the depth, and less than 30% for the thermal resistance (see Figure 11). The values of accuracy here given are intrinsic to the method and do not include the influence of the experimental noise and the 3D heat transfer effect linked to the limited extent of defects. The experimental noise can be reduced with the modern thermographic cameras characterized by an NETD of 20 mK or less, and by the use of a preprocessing technique of the thermograms such as the TSR method (see following Section).

4.3.2. Improvement of the Emerging Contrast Technique by the Combined Use of the Thermographic Signal Reconstruction Technique (TSR). The TSR method [33–37], well known and largely used in pulse thermographic NDE, consists in the fitting of the experimental log-log plot thermogram by a logarithmic polynomial

$$\ln(\Delta T) = a_0 + a_1 \ln(t) + a_2[\ln(t)]^2 \cdots + a_n[\ln(t)]^n, \quad (10)$$

and the use for NDE purpose of the 1st and 2nd logarithmic derivatives of the thermogram, the derivation being achieved directly on the polynomial, then with a limited increase of the temporal noise.

The advantages of the fitting are as follows: (i) a noticeable noise reduction; (ii) the replacement of the sequence of temperature rise images, $\Delta T(i, j, t)$, by the series of $(n + 1)$ images of the polynomial coefficients,

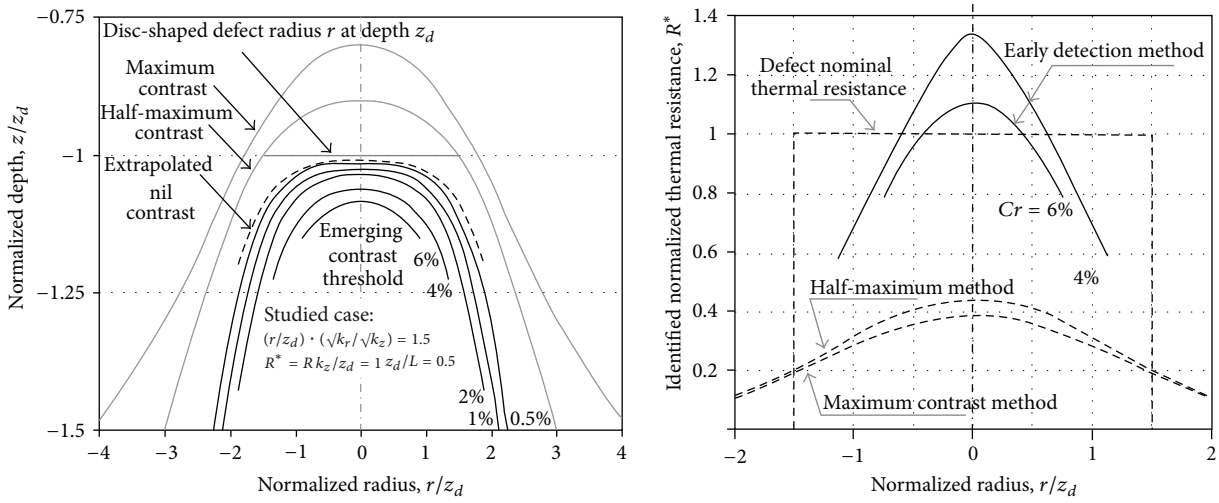

Figure 11: Simulation results: (a) identification of the depth profile of a circular defect ($r_d/z_d = 1.5$ and $R_d{}^* = R_d k_z/z_d = 1$) using the early detection/characterization with extrapolation to zero contrast and comparison to the results obtained with the maximum and half maximum contrast techniques (simulation results taken from Krapez and Balageas [18]), revisited using a linear extrapolation [19, 20]; (b) identification of the thermal resistance profile, taken from [20].

$a_0(i, j), \ldots, a_n(i, j)$, which allows a drastic reduction of the data amount; (iii) the possibility of reconstructing a full thermographic sequence (from which the name of the method follows).

The logarithmic derivations are interesting too, because they produce a remarkable increase of detectivity and a "precession" of the detection [19, 20], which improve the precociousness of the defect detection.

So, it is easy to understand that both methods (early detection by emerging contrast and TSR) pursue identical purposes, and that consequently coupling them is beneficial. The increase of signal-to-noise ratio (SNR) given by the logarithmic fitting is particularly welcome since experimental crude thermal contrasts may have weak SNR, especially when deep defects are considered. In this case, the TSR technique is used as a preprocessing tool before application of the early detection process. An example of such a coupling is shown in [20].

A deeper coupling could be used, consisting in considering the emerging contrast of the 1st or 2nd logarithmic derivatives instead of the emerging contrast of the thermogram itself for the characterisation of the defect. Such an early detection method, which remains until now to be established regarding the quantitative identification of the defect parameters, is better than the one based on the half-rise time of the first derivative or the time of the maximum of the second derivative. Nevertheless, if the sole qualitative aspect is considered (detection of defects from thermographic images), the use of early images of the first and second logarithmic derivatives produces sharper defect images, a noticeable improvement compared to traditional maximum contrast images. Figure 12, taken from [19], demonstrates the ability of this approach to produce images with good SNR and high sharpness, making the pulse thermographic NDE technique comparable to the better-established techniques, in particular ultrasonics.

4.3.3. Application of the Early Detection and Characterization of Defects to Step-Heating Thermography. The early detection and characterization approach based on the emerging contrast has been extended to step-heating thermography, leading to comparable improvements. The theory is given in [38], leading to identification formulas for defect depth and thermal resistance analogous to the ones found for pulse heating experiments (8).

5. Conclusion and Perspectives

A review of the literature of the early time detection approach in the field of thermophysical properties measurements and NDE has been made.

This approach has been built progressively and never presented as a well-defined general procedure. This is due to the fact that the applications of the method were spread in time (3 decades) and pertaining to different fields. Putting these works in perspective, it has been possible to describe and formalize the general procedure here called "the early detection and characterization."

In the field of thermophysical properties measurements, two examples of flash diffusivity identification using rear face thermograms have been presented. They illustrate the philosophy of the approach and are well suited to thermography.

This paper demonstrates that in NDE by pulse-stimulated thermography, the generally followed attitude that consists in taking into account the sole signal-to-noise ratio when optimizing an identification process is an error. The optimization

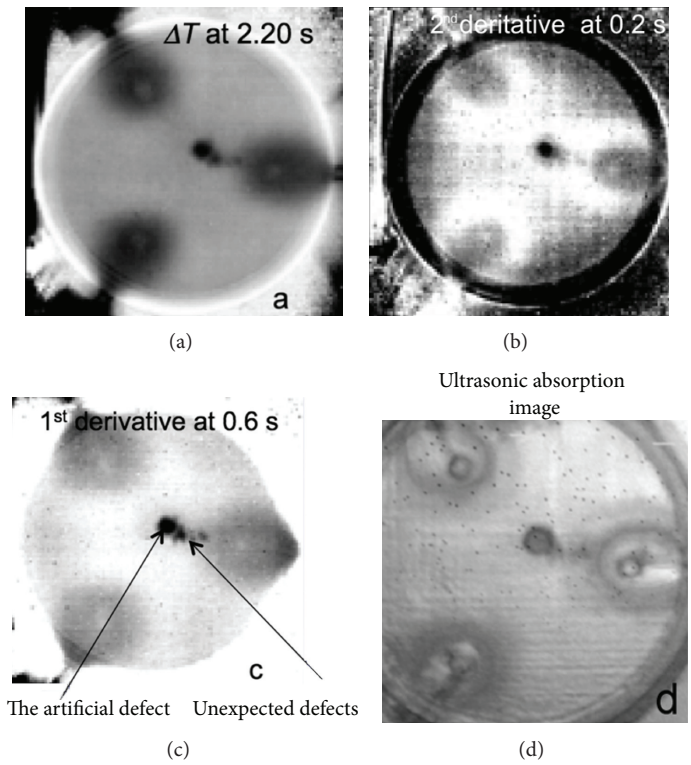

Figure 12: Comparison between the best images obtained by the TSR method coupled with an early detection approach and an ultrasonic D-scan: (a) Thermograms, ΔT at 2.20 s; (b) 2nd derivative at 0.20 s; (c) 1st derivative at 0.6 s; (d) ultrasonic absorption image. The artificial defect to detect is located at the center of the sample. Unexpected defects were discovered in the near vicinity of the artificial defect. The chosen times of observation have not been optimized for imaging the 3 peripheral inner inserts that are sound regions.

must consider with the same weight the signal-to-noise ratio and the precociousness for both qualitative and quantitative purposes.

A way to conciliate both signal-to-noise ratio and precociousness is now more easily feasible by combining the early detection/characterization and the thermographic signal reconstruction (TSR) technique. Presently, this combination has given rise to recent developments in the field of NDE, increasing the attractiveness of time-resolved thermography.

References

[1] R. B. Orlande, O. Fudym, D. Maillet, and R. M. Cotta, Eds., *Thermal Measurements and Inverse Techniques*, CRC Press, 2011.

[2] W. J. Parker, R. J. Jenkins, C. P. Butler, and G. L. et Abbot, "Flash method of determining thermal diffusivity, heat capacity and thermal conductivity," *Journal of Applied Physics*, vol. 32, no. 9, pp. 1679–1684, 1961.

[3] D. Balageas, "Flash Thermal diffusivity measurements using a novel temperature-time history analysis," in *Proceedings of the 1st International Joint Conferences on Thermophysical Properties*, no. TP 1981-62, ONERA, Gaithersburg, Md, USA, June 1981.

[4] D. L. Balageas, "Nouvelle méthode d'interprétation des thermogrammes pour la détermination de la diffusivité thermique par la méthode impulsionnelle (méthode flash)," *Revue de Physique Appliquée*, vol. 17, pp. 227–237, 1982 (French).

[5] A. Degiovanni, "Diffusivité et méthode flash," *Revue Générale de Thermique*, vol. 16, no. 185, pp. 420–442, 1977 (French).

[6] A. Degiovanni, "Identification de la diffusivité thermique par l'utilisation des moments temporels partiels," *High Temperatures-High Pressures*, vol. 17, pp. 683–689, 1985 (French).

[7] D. L. Balageas and A. M. Luc, "Transient thermal behavior of directional reinforced composites: applicability limits of homogeneous property model," *AIAA Journal*, vol. 24, no. 1, pp. 109–114, 1986.

[8] A. M. Luc and D. L. Balageas, "Non-stationary thermal behavior of reinforced composites—a better evaluation of wall energy balance for convective conditions," in *Proceedings of the 1st International Joint Conferences on Thermophysical Properties*, no. TP 1981-61, ONERA, Gaitherburg, Md, USA, June 1981.

[9] A. M. Luc-Bouhali, R. M. Pujolà, and D. L. Balageas, "Thermal diffusivity in situ measurements of carbon/carbon composite reinforcements," in *Thermal Conductivity*, T. Ashworth and D. R. Smith, Eds., vol. 18, pp. 613–624, Plenum, London, UK, 1984.

[10] R. M. Pujolà and D. L. Balageas, "Derniers développements de la méthode flash adaptée aux matériaux composites à renforcement orienté," *High Temperature-High Pressure*, vol. 17, pp. 623–632, 1985 (French).

[11] D. L. Balageas, "Détermination par méthode flash des propriétés thermiques des constituants d'un composite à renforcement orienté," *High Temperatures-High Pressures*, vol. 16, pp. 199–208, 1984 (French).

[12] D. L. Balageas, "Détermination de la diffusivité thermique du milieu homogène équivalent à un matériau composite à renforcement orienté," *Comptes-Rendus des Séances de l'Académie des Sciences*, vol. 299, no. 4, pp. 143–148, 1984 (French).

[13] J.-P. Bardon, D. Balageas, A. Degiovanni, and J. Vuiiliermes, "Thermics of composites and interfaces: current status and perspectives," *La Recherche Aérospatiale*, no. 1989-6, pp. 37–45, 1989.

[14] D. Balageas, A. Déom, and D. Boscher, "Composite thermal properties measurements by pulse photothermal radiometry," in *Proceedings of the Eurotherm IV Conference Thermal Transfer in Composite Materials and Solid-Solid Interface*, pp. 92–95, Nancy, France, June-July 1988.

[15] J. C. Krapez, *Contribution à la caractérisation des défauts de type délaminage ou cavité par thermographie stimulée [Ph.D. thesis]*, Ecole Centrale de Paris, Châtenay-Malabry, France, 1991.

[16] D. L. Balageas, J. C. Krapez, and P. Cielo, "Pulsed photothermal modeling of layered materials," *Journal of Applied Physics*, vol. 59, no. 2, pp. 348–357, 1986.

[17] D. L. Balageas, A. A. Deom, and D. M. Boscher, "Characterization and nondestructive testing of carbon-epoxy composites by a pulsed photothermal method," *Materials Evaluation*, vol. 45, no. 4, pp. 461–465, 1987.

[18] J. C. Krapez and D. Balageas, "Early detection of thermal contrast in pulsed stimulated infrared thermography," in *Proceedings of the Quantitative Infrared Thermography, Editions Europ Thermosonde et Induction (QIRT '94)*, pp. 260–266, 1994, http://qirt.gel.ulaval.ca/dynamique/index.php?idD=56, paper # QIRT 1994-039.

[19] D. L. Balageas, "Defense and illustration of time-resolved thermography for NDE," in *Proceedings of the SPIE Thermosense III*, vol. 8013, pp. 8013V-1–88013V20, 2011, http://publications.onera.fr/exl-php/cadcgp.php.

[20] D. Balageas, "Defense and illustration of time-resolved thermography for NDE," *Quantitative InfraRed Thermography Journal*, vol. 9, no. 1, pp. 5–38, 2012.

[21] J. Bontaz, Ch. Fort, and B. Horbette, "Identification de la profondeur et de la valeur de la résistance thermique de contact dans des matériaux stratifiés par la méthode photothermique impulsionnelle," in *Proceedings of the Annual Conference of the Société Française des Thermiciens (SFT '90)*, pp. 221–224, Nantes, France, May 1990.

[22] J. Bontaz, *Une méthode photothermique impulsionnelle appliquée au contrôle de matériaux composites [Ph.D. thesis]*, University of Bordeaux, 1991.

[23] D. L. Balageas, D. M. Boscher, and A. A. Déom, *Temporal Moment Method in Pulsed Photothermal Radiometry. Application to Carbon Epoxy N.D.T.*, vol. 58 of *Springer Series in Optical Sciences*, Springer, 1987.

[24] J. C. Krapez, D. Balageas, A. Deom, and F. Lepoutre, "Early detection by stimulated infrared thermo-graphy. Comparison with ultrasonics and holo/shearo-graphy," in *Advances in Signal Processing for Non Destructive Evaluation of Materials*, X. P. V. Maldague, Ed., vol. 262 of *NATO ASI Series E*, pp. 303–321, Kluwer Academic, 1994.

[25] J.-C Krapez, F. Lepoutre, and D. Balageas, "Early detection of thermal contrast in pulsed stimulated thermography," *Journal de Physique IV*, vol. 4, no. C7, pp. 47–50, 1994.

[26] S. K. Lau, D. P. Almond, and J. M. Milne, "A quantitative analysis of pulsed video thermography," *NDT and E International*, vol. 24, no. 4, pp. 195–202, 1991.

[27] D. P. Almond and S. K. Lau, "A quantitative analysis of pulsed video thermography," in *Proceedings of the Quantitative Infrared Thermography, Editions Europ Thermosonde et Induction (QIRT '92)*, pp. 207–211, QIRT, Paris, France, 1992, http://qirt.gel.ulaval.ca/dynamique/index.php?idD=55, paper # QIRT, 1992-031.

[28] L. D. Favro, X. Han, P. K. Kuo, and R. L. Thomas, "Imaging the early time behavior of reflected thermal wave pulses," in *Proceedings of the Thermosense XVII: An International Conference on Thermal Sensing and Imaging Diagnostic Applications*, pp. 162–166, April 1995.

[29] X. Han, L. D. Favro, P. K. Kuo, and R. L. Thomas, "Early-time pulse-echo thermal wave imaging," *Review of Progress in Quantitative Nondestructive Evaluation*, vol. 15, pp. 519–524, 1996.

[30] R. L. Thomas, L. D. Favro, and P. K. Kuo, "Thermal wave imaging of hidden corrosion in aircraft components," Report AFOSR-TR-96, 1996.

[31] H. I. Ringermacher et al., "Towards a flat-bottom hole standard for thermal imaging," in *Review of Progress in Quantitative Nondestructive Evaluation*, D. O. Thompson and D. E. Chimenti, Eds., vol. 17, pp. 425–429, Plenum Press, New York, NY, USA, 1998.

[32] J. G. Sun, "Analysis of pulsed thermography methods for detect depth prediction," *Journal of Heat Transfer*, vol. 128, no. 4, pp. 329–338, 2006.

[33] S. M. Shepard, T. Ahmed, B. A. Rubadeux, D. Wang, and J. R. Lhota, "Synthetic processing of pulsed thermographic data for inspection of turbine components," *Insight*, vol. 43, no. 9, pp. 587–589, 2001.

[34] S. M. Shepard, J. R. Lhota, B. A. Rubadeux, D. Wang, and T. Ahmed, "Reconstruction and enhancement of active thermographic image sequences," *Optical Engineering*, vol. 42, no. 5, pp. 1337–1342, 2003.

[35] S. M. Shepard, Y. L. Hou, T. Ahmed, and J. R. Lhota, "Reference-free interpretation of flash thermography data," *Insight*, vol. 48, no. 5, pp. 298–307, 2006.

[36] S. M. Shepard, J. Hou, J. R. Lhota, and J. M. Golden, "Automated processing of thermographic derivatives for quality assurance," *Optical Engineering*, vol. 46, no. 5, Article ID 051008, 2007.

[37] S. M. Shepard, "Flash thermography of aerospace composites," in *Proceedings of the 4th Pan American Conference for NDT*, Buenos Aires, Argentina, October 2007, http://www.ndt.net/article/panndt2007/papers/132.pdf.

[38] D. Balageas and J. M. Roche, "Détection précoce et caractérisation de défauts par thermographie stimulée par échelon de flux et comparaison à la méthode impulsionnelle," in *Congrès Annuel de la Société Française de Thermique*, Bordeaux, France, May-June 2012, http://publications.onera.fr/exl-doc/DOC401721_s1.pdf .